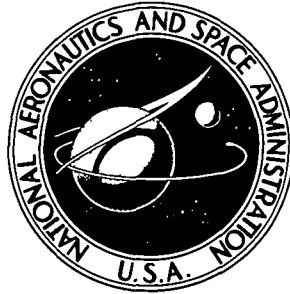


NASA TECHNICAL NOTE



N73-32148  
NASA TN D-7338

NASA TN D-7338

CASE FILE  
COPY

INVESTIGATION OF RESPONSIVITY  
AND NOISE IN A DIRECT-COUPLED  
PHOTODETECTOR-PREAMPLIFIER  
FOR FACSIMILE CAMERAS

*by W. Lane Kelly IV and Stephen J. Katzberg*

*Langley Research Center*

*Hampton, Va. 23665*

|   |  |  |  |
|---|--|--|--|
| 1 Report No<br>NASA TN D-7338   | 2 Government Accession No                          | 3 Recipient's Catalog No   |  |
| 4 Title and Subtitle<br>INVESTIGATION OF RESPONSIVITY AND NOISE IN A<br>DIRECT-COUPLED PHOTODETECTOR-PREAMPLIFIER<br>FOR FACSIMILE CAMERAS  |  | 5 Report Date<br>October 1973  | 6 Performing Organization Code                   |
|   |  | 8 Performing Organization Report No<br>L-9000  | 10 Work Unit No<br>502-03-52-04                  |
| 7 Author(s)<br>W Lane Kelly IV and Stephen J. Katzberg  |  | 11 Contract or Grant No  |  |
|   |  | 13 Type of Report and Period Covered<br>Technical Note   |  |
| 9 Performing Organization Name and Address<br>NASA Langley Research Center<br>Hampton, Va. 23665  |  | 14 Sponsoring Agency Code  |  |
|   |  | 12 Sponsoring Agency Name and Address<br>National Aeronautics and Space Administration<br>Washington, D.C. 20546 |  |
| 15 Supplementary Notes  |  |  |  |
| 16 Abstract<br><br>The direct-coupled (DC) mode of detector operation is evaluated for use in a facsimile camera. Photodiode-preamplifier sensitivity is described in terms of photodiode responsivity and possible noise sources resulting from the photodiode and preamplifier. Responsivity and noise limitations are experimentally verified and used to predict photodiode-preamplifier sensitivity under a wide range of operating conditions. Results demonstrate that the DC mode offers advantages in sensitivity and reduced mechanical complexity for facsimile cameras over the more common technique of chopping the radiation and ac amplifying the resultant signal. |  |  |  |
| 17 Key Words (Suggested by Author(s))<br>Photodiode-preamplifier<br>Facsimile camera<br>Direct coupled<br>Sensitivity<br>Responsivity<br>Noise  |  | 18 Distribution Statement<br>Unclassified - Unlimited  |  |
| 19 Security Classif (of this report)<br>Unclassified  | 20 Security Classif (of this page)<br>Unclassified | 21 No of Pages<br>23   | 22 Price*<br>Domestic, \$2.75<br>Foreign, \$5.25 |

INVESTIGATION OF RESPONSIVITY AND NOISE  
IN A DIRECT-COUPLED PHOTODETECTOR-PREAMPLIFIER  
FOR FACSIMILE CAMERAS

By W. Lane Kelly IV and Stephen J. Katzberg  
Langley Research Center

SUMMARY

The direct-coupled (DC) mode of detector operation is evaluated for use in a facsimile camera. Photodiode-preamplifier sensitivity is described in terms of photodiode responsivity and possible noise sources resulting from the photodiode and preamplifier. Responsivity and noise limitations are experimentally verified and used to predict photodiode-preamplifier sensitivity under a wide range of operating conditions. Results demonstrate that the DC mode offers advantages in sensitivity and reduced mechanical complexity for facsimile cameras over the more common technique of chopping the radiation and ac amplifying the resultant signal.

INTRODUCTION

A facsimile camera, or optical-mechanical scanner, has been chosen to provide imagery data from the Mars Viking lander scheduled to be flown in 1975. The important parameters which determine the image quality from a facsimile camera are the depth of field, angular resolution, and signal-to-noise ratio. As determined in reference 1, these parameters are so interrelated that only an improvement in the sensitivity of the photon detection technique can lead to significant improvements in camera performance for a planetary lander configuration. The silicon photodiode was selected for the facsimile camera photodetector because of its small size, high sensitivity, and spectral response in the visual region, and is therefore considered in this paper.

The sensitivity of the photon detection technique is determined by the photodiode responsivity and the noise generated by the photodiode and preamplifier. The photon detection technique generally employed consists of mechanically chopping the incoming radiation and ac amplifying the video signal. This technique has the advantage of placing the video signal higher on the frequency spectrum and thus avoiding dc offsets, drift, and  $1/f$  noise. For a detector-noise-limited case the disadvantages include a loss of energy proportional to the chopping duty cycle (typically 50 percent), an additional bandwidth

requirement for the preamplifier, and an increase in mechanical complexity, which affects system reliability.

Neither the tuning fork chopper nor a rotating aperture wheel provides attractive chopping schemes. The tuning fork chopper is limited to a chopping frequency of approximately 3 kHz (ref. 2), which is too low for the photosensor aperture sizes required for the Viking camera, for example. Because the rotating aperture wheel requires a small motor, it has obvious disadvantages for a system constrained by size, power, and weight. In addition, both schemes provide primary failure modes, since chopper failure could completely obscure the incoming radiation or at best shift the frequency range beyond that of the demodulation circuitry. These considerations led to an investigation of the direct-coupled (DC) mode of detector operation and its adaptability to the facsimile camera.

This paper presents an analytical and experimental evaluation of the DC mode of operation which considers characterization of noise sources and detector-preamplifier design for operation with minimum noise and maximum sensitivity. A drift control technique, made possible by the unique operation of the facsimile camera, is shown to reduce the effects of dc offsets, drift, and  $1/f$  noise originating in the photodiode and preamplifier, thus providing a lower frequency limit for the noise bandwidth. Sensitivity of this design is predicted and experimentally verified for a range of facsimile camera operating conditions.

## SYMBOLS

|               |   |
|---------------|---|
| A             | amplifier gain  |
| $A_D$         | detector area, $m^2$                                    |
| $C_f$         | feedback capacitance, F                                 |
| c             | velocity of light, m/sec                                |
| D             | lens diameter, m  |
| $D_\lambda^*$ | spectral detectivity of detector, $m\text{-Hz}^{1/2}/W$ |
| $E_{Jn}$      | rms Johnson noise voltage, V                            |
| $F(\alpha)$   | dimensionless function of absorption coefficient        |

|                 |   |
|-----------------|---|
| $f$             | frequency, Hz                                     |
| $f_c$           | 3-dB cutoff frequency, Hz                         |
| $f_o$           | low-frequency cutoff of video bandwidth, Hz       |
| $g_m$           | channel conductance, S                            |
| $H_\lambda$     | spectral irradiance, W/m <sup>2</sup> - $\mu$ m   |
| $h$             | Planck's constant                                 |
| $I_{dc}$        | photodiode dark current, A                        |
| $I_n$           | rms noise current, A                              |
| $I_s$           | signal current, A                                 |
| $I_t$           | rms total noise current from all noise sources, A |
| $\bar{i}_{Jn}$  | rms Johnson noise current, A                      |
| $\bar{i}_{sn}$  | rms shot noise current, A                         |
| $\bar{i}_{1/f}$ | rms 1/f noise current, A                          |
| $J_o$           | photocurrent density, A/m <sup>2</sup>            |
| $j = \sqrt{-1}$ |   |
| $k$             | Boltzmann's constant                              |
| $L$             | diffusion length, cm                              |
| $q$             | electronic charge, C                              |
| $R_f$           | feedback resistance, $\Omega$                     |
| $R_g$           | gain setting resistance, $\Omega$                 |

|             |  |
|-------------|--|
| $R_L$       | load resistance, $\Omega$  |
| $R_\lambda$ | spectral responsivity of detector, A/W   |
| S/N         | average signal-to-rms-noise ratio  |
| $S_\lambda$ | solar irradiance above Martian atmosphere, $W/m^2-\mu m$                           |
| T           | absolute temperature, K  |
| $t_d$       | dwelt time of each scan element, sec   |
| $t_f$       | time allotted for frame, sec   |
| $t_v$       | time interval between dark sampling and completion of succeeding scan line,<br>sec |
| $V_o$       | preamplifier output voltage, V   |
| W           | bandwidth, Hz  |
| $\alpha$    | absorption coefficient, $cm^{-1}$  |
| $\beta$     | angular scanning resolution, deg   |
| $\delta$    | constant   |
| $\eta$      | scanning efficiency  |
| $\theta_h$  | horizontal field of view, deg  |
| $\theta_v$  | vertical field of view, deg  |
| $\lambda$   | wavelength, $\mu m$  |
| $\nu$       | radiant frequency, Hz  |
| $\rho$      | reflectivity   |

|                    |  |
|--------------------|--|
| $\rho_\lambda$     | spectral reflectivity of surface (normal albedo)                             |
| $\sigma$           | dimensionless gain constant  |
| $\tau_\lambda$     | spectral transmissivity of atmosphere  |
| $\tau_{\lambda,L}$ | spectral transmissivity of optics  |
| $\Phi$             | photon flux rate, photons/sec-m <sup>2</sup>                                 |
| $\phi$             | illumination scattering function   |
| $\Delta\phi$       | difference in illumination scattering function between object and background |
| $\psi$             | constant   |
| $\Omega$           | incident radiant power density, W/m <sup>2</sup>                             |

## ANALYSIS

The facsimile camera consists of a radiometer and a scanning mechanism, as shown in figure 1. The objective lens of the radiometer focuses light from the scene onto a detector. A vertically scanning mirror on the object side of the lens allows the radiometer to scan a vertical field, and the entire assembly is rotated slowly in azimuth to generate contiguous vertical scan lines. The direct-coupled (DC) mode of detector-preamplifier operation to be considered here consists of dc amplification of the detector output with dark reference sampling between scan lines to reduce the effects of dc offsets and drift. The video signal is further processed, digitized, and transmitted for image reconstruction. The reconstruction process consists of imaging a light source modulated by the video signal onto a storage medium such as film and scanning the image in a manner identical with the camera scan.

The following section will define the detector characteristic which determines the signal current, describe the possible noise sources, define the noise bandwidth, and present a design which affords optimum signal-to-noise ratio over a wide range of operating conditions.

### Signal-to-Noise Ratio

The signal-to-noise ratio for the facsimile camera can be expressed as (ref. 1)

$$\frac{S}{N} = \frac{\pi\beta^2 D^2 \Delta\phi}{5.25 \times 10^4 \sqrt{A_D W}} \int_0^\infty S_\lambda \tau_{\lambda\rho} \tau_{\lambda,L} D_\lambda^* d\lambda \quad (1)$$

This expression makes use of the photodetector detectivity  $D_\lambda^*$  to specify the system signal-to-noise ratio. However, in the case of the facsimile camera, the ultimate photodetector sensitivity is difficult to realize for two reasons: Firstly, even with optimum design, the preamplifier may introduce noise equal to or greater than the detector noise. Secondly, as video bandwidth requirements increase, the noise generated from the preamplifier also increases. In order to include additional noise sources, the expression for system signal-to-noise ratio can better be written in terms of detector responsivity and the total noise current. From the definition of detectivity  $D_\lambda^*$  (ref. 3)

$$D_\lambda^* = \frac{I_S(W)^{1/2}}{I_n H_\lambda (A_D)^{1/2}} \quad (2)$$

and responsivity  $R_\lambda$  (ref. 3)

$$R_\lambda = \frac{I_S}{H_\lambda A_D} \quad (3)$$

the two parameters can be related by

$$D_\lambda^* = \frac{R_\lambda (A_D W)^{1/2}}{I_n} \quad (4)$$

Replacing  $D_\lambda^*$  in equation (1) results in

$$\frac{S}{N} = \frac{\pi\beta^2 D^2 \Delta\phi}{5.25 \times 10^4 I_t} \int_0^\infty S_\lambda \tau_{\lambda\rho} \tau_{\lambda,L} R_\lambda d\lambda \quad (5)$$

The diode noise current has been replaced by the total rms noise current from all noise sources over the total noise bandwidth. This expression defines the dependence of the signal-to-noise ratio on the detector-preamplifier performance, to be considered here in terms of detector responsivity  $R_\lambda$  and the total noise current  $I_t$ .



## Responsivity

The responsivity of photodiodes is a direct result of the absorption of photons from incident radiation to create hole-electron pairs. The efficiency with which these carriers (holes or electrons) are converted into an electric current is a function of several parameters, some of which are associated with the semiconductor material and others which are related to the particular diode structure. For a certain incident radiant power density  $\Omega$ , quantum theory predicts an incident flux rate of

$$\Phi = (1 - \rho) \frac{\lambda}{hc} \Omega \quad (6)$$

where  $(1 - \rho)$  is the optical absorption;  $\lambda$ , the light wavelength;  $h$ , Planck's constant; and  $c$ , the velocity of light.

If each photon is absorbed in a band-to-band process, a hole-electron pair is generated. In a diode, a hole or an electron will be a minority carrier, and its collection at the depletion region in a reverse-biased diode will result in an increased current which can be detected and amplified. Sawyer and Rediker (ref. 4) analyzed one diode structure with the following result:

$$J_0 = q\Phi F(\alpha) \quad (7)$$

where  $J_0$  is the photocurrent density,  $q$  is the electronic charge, and  $F(\alpha)$  is a complicated function of the optical absorption constant. This function has a maximum value of 1.0 but is strongly dependent on  $\alpha$ . As an approximation  $F(\alpha)$  may be written

$$F(\alpha) \approx \frac{\alpha^2 L^2}{\alpha^2 L^2 - 1} \quad (\alpha L > 1) \quad (8)$$

where  $L$  is the minority-carrier diffusion length. The responsivity of the diode is then

$$R_\lambda = \frac{J_0}{\Omega} = q \frac{1 - \rho}{h\nu} \frac{\alpha^2 L^2}{\alpha^2 L^2 - 1} \quad (9)$$

which is valid only for  $\alpha L > 1$ .

Evaluating equation (9) for  $\lambda \approx 0.8 \mu\text{m}$  gives

$$R_\lambda \approx \frac{2}{3} (1 - \rho) \quad (10)$$

The factor  $(1 - \rho)$  is approximately 0.7 (ref. 5) to yield

$$R_\lambda \approx 0.46 \text{ A/W at } \lambda = 0.8 \text{ } \mu\text{m} \quad (11)$$

The value of  $R_\lambda$  at approximately  $0.8 \text{ } \mu\text{m}$  represents the peak response for a silicon photodiode. The response for shorter wavelength radiation decreases for two general reasons. First, the reflectivity coefficient increases with a resulting decrease in the number of hole-electron pairs generated. Second, the shorter wavelength radiation is absorbed within approximately  $1.0 \text{ } \mu\text{m}$  of the surface. Defects in the surface reduce the lifetime in this region; consequently, carriers recombine before they can be collected at the junction and contribute to the photocurrent.

In the longer wavelength region beyond the peak response, the absorption coefficient decreases and longer optical path lengths are required if hole-electron pairs are to be produced. In order to improve the collection efficiency of these carriers, the PIN structure, which consists of a wide intrinsic region between the P and N regions, is used to provide the longer optical path for longer wavelength radiation. A reverse bias applies an electric field across the entire intrinsic region to aid carriers in reaching the junction to contribute to the photocurrent. Finally, as the wavelength continues to increase, sufficient energy is not available to excite carriers across the forbidden gap and, therefore, no photocurrent is generated.

#### Minimum Noise Condition

In order to illustrate the characterization of the noise and the preamplifier design for minimum noise operation, consider a typical diode-amplifier combination, as shown in figure 2. The diode is reverse biased and drives a typical current-to-voltage converter. The input stage of the amplifier is a low-noise, field-effect transistor (FET) with a high input impedance. The generality of the circuit may be seen by the following values for the gain constant  $\sigma$ , and the amplifier gain  $A$ : If  $\sigma = 0$  and  $A$  is unity or greater, the diode-amplifier combination reduces to nothing more than a diode with a load resistor, the simplest measuring device. If  $\sigma > 0$  and  $A$  is large and negative, the wide-band diode-preamplifier required to transform the impedance and maintain a high bandwidth capability is obtained.

The current-to-voltage converter. - This last configuration, with large negative  $A$  and  $\sigma > 0$ , is called a current-to-voltage converter. (See, e.g., ref. 6.) This terminology is based on the following fact: The photodiode, which can be represented as a current source, feeds directly into the input node of the preamplifier. If the diode has a light-generated current  $I_S$ , then the preamplifier output voltage is

$$V_o = \frac{1}{\sigma} I_s R_f \frac{1}{1 + 2\pi j R_f C_f f} \quad (R_f \gg R_g) \quad (12)$$

The static or dc response of this configuration is  $\frac{1}{\sigma} I_s R_f$ , while its frequency response is that of a single-pole low-pass filter with a 3-dB cutoff frequency:

$$f_c = \frac{1}{2\pi R_f C_f} \quad (13)$$

where  $C_f$  is the parasitic capacitance in parallel with the feedback resistance.

Equation (13) adequately represents the electrical characteristics of the current-to-voltage converter so long as the time constant  $R_f C_f$  is greater than or equal to  $R_{in} C_{in}$ , the parallel combination of input capacitance and resistance. (See ref. 6.) In the cases to be presented herein, this condition is always satisfied.

Noise sources. - Several noise sources must be considered as possible contributing factors in the total noise current. These noise sources are as follows: (1) shot noise from the photodiode, (2) Johnson or thermal noise from the feedback resistor, (3) flicker or 1/f noise, (4) amplifier noise, (5) drift from photodiode and amplifier due to environmental conditions, and (6) photon background noise. The photon-noise-limited detectivity in the wavelength region of silicon detector response is several orders of magnitude above the limit imposed by the diode shot noise (ref. 7); consequently, photon noise will not be considered herein.

The shot noise of the photodiode is analogous to the shot noise in vacuum tubes resulting from the random arrival of individual electrons at the anode. In the photodiode, carriers which have been thermally generated pass across the junction by diffusion, comprising the diode dark leakage current  $I_{dc}$ . Shot noise is generated by these independent carriers according to the relation

$$\bar{i}_{sn}^2 = 2qI_{dc}W \quad (14)$$

where  $q$  is electronic charge and  $W$  bandwidth. Attempts to minimize the shot noise consist of reducing the dark leakage current. The leakage current is proportional to the junction area, indicating that a small detector must be used. However, surface leakage contributes to the total leakage current and may become significant as the junction area is greatly reduced (ref. 8).

Johnson or thermal noise results from the random movement of electrons in the feedback resistor. In accordance with the kinetic theory of heat, the electrons in a con-

ductor are in continual random motion in thermal equilibrium with the molecules. The resultant noise current is

$$\bar{i}_{Jn}^2 = \frac{4kTW}{R_L} \quad (15)$$

where  $k$  is Boltzmann's constant,  $W$  is bandwidth, and  $T$  is the absolute temperature (ref. 9). A large decrease in temperature is required in order to produce a significant reduction in the Johnson noise. It should be noted at this point that both Johnson noise and shot noise are functions of bandwidth but not of frequency (white noise).

The dominant source of noise at low frequencies in both the FET preamplifier input and photodiode is flicker noise, also known as  $1/f$  and current noise. Flicker noise is characterized by a  $1/f$  power dependence, and is described by

$$\bar{i}_{1/f}^2 = \int_{f_1}^{f_2} \frac{Y^2 I_{dc}^\delta}{f^\psi} df \quad (16)$$

where  $Y$  is a proportionality factor,  $\delta$  and  $\psi$  are constants that depend on the device, and  $f_1$  and  $f_2$  define the band over which the noise is measured. Typical values of  $\delta$  and  $\psi$  are 2 and 1, respectively; thus the  $1/f$  noise current is

$$\bar{i}_{1/f}^2 = Y^2 I_{dc}^2 \ln \frac{f_2}{f_1} \quad (17)$$

where  $Y I_{dc}$  is the rms noise current per hertz<sup>1/2</sup> at 1 hertz. This expression indicates an infinite amount of noise unless the frequency bandwidth is limited; consequently, this  $1/f$  relation does not hold over all frequencies. However, this dependence has been observed over many frequency decades extending to 0.2 mHz (ref. 7).

Amplifier noise results from the input FET and can be considered as having two sources. First, the gate leakage current, typically a few picoamperes, produces shot noise. For the purpose of noise calculations the gate leakage current and the diode leakage current may be summed to determine the resulting total shot noise. Second, the conducting channel of the FET also generates Johnson or thermal noise,

$$\bar{E}_{Jn}^2 = \frac{4kTW}{g_m} \quad (18)$$

where  $g_m$  is the FET channel conductance (ref. 10). For normal video-bandwidth requirements the value of load resistance is sufficiently high to convert the input noise currents into noise voltages far exceeding the Johnson noise from the channel conductance. Therefore, for typical values of  $g_m$  ( $70 \mu S$ ) this noise source can be neglected for bandwidths below approximately 500 kHz.

Amplifier drift must also be considered as a potential noise source at very low frequencies. Temperature stabilization and proper operation of drift-control circuitry to provide a lower limit to the noise bandwidth should eliminate this noise source from consideration. The total noise current can be determined by evaluation of each noise source over the noise bandwidth and summing them as follows (ref. 11):

$$I_t = \left( i_{sn}^2 + i_{Jn}^2 + i_{1/f}^2 \right)^{1/2} \quad (19)$$

Noise bandwidth. - Determination of the total noise current requires a knowledge of the noise bandwidth under operating conditions. The upper frequency limit for facsimile cameras has been derived in reference 1 as

$$f_c = \frac{1}{2t_d} = \frac{\theta_h \theta_v}{2\beta^2 \eta t_f} \quad (20)$$

where  $t_d$  is the dwell time of each scan element,  $\theta_h$  and  $\theta_v$  are the horizontal and vertical fields of view,  $\eta$  is the scan efficiency, and  $t_f$  is the time allotted per frame. The factor 2 appears in the denominator since a Nyquist sampling rate is assumed. For a single-pole, low-pass filter having a 3-dB cutoff frequency given by equation (13), the noise-equivalent bandwidth is

$$\frac{\pi}{2} f_c = \frac{1}{4R_f C_f} \quad (21)$$

where  $R_f$  is the feedback resistance and  $C_f$  is the parallel feedback capacitance.

During data acquisition the video processing electronics must have essentially dc response to allow for the possibility of scanning a large area of uniform intensity without loss of radiometric accuracy. It is desirable therefore to direct-couple the video information; unfortunately, this allows drift, changes in bias, and 1/f noise to become significant noise sources at low frequencies.

To reduce the effects of these sources, the preamplifier output is coupled to a drift-control circuit, illustrated in figure 3. Operation consists of sampling the preamplifier

output while the mirror is looking away from the scene (dark condition) and subtracting any dc offsets from the next succeeding scan line, thus reducing the effect of very low-frequency noise. The analysis of this circuit operation is treated in reference 12, and only the result is stated herein. Drift-control circuitry may be modeled as a high-pass filter with a cutoff frequency, typically below 100 Hz, which is defined by

$$f_0 = \frac{1}{40t_v} \approx \frac{\beta}{40t_d\theta_v} \quad (22)$$

where  $t_v$  is the time interval between dark sampling and completion of the succeeding scan line.

Noise spectrum.- To illustrate the important noise sources and the resulting influence on the preamplifier design, a typical noise spectrum is shown in figure 4. At low frequencies the noise spectrum is dominated by  $1/f$  noise from the photodiode and the FET. The magnitude of  $1/f$  noise varies significantly from one device to another and the curve utilized may be considered conservative.

The flat region of the noise spectrum is composed of both Johnson noise and shot noise, both of which are frequency independent. Generally this region will be dominated by shot noise until the upper frequency requirement necessitates a decrease in feedback resistance to the point where Johnson noise dominates. The noise spectrum begins to roll off at higher frequencies because of the preamplifier frequency response, determined by the feedback resistance and input capacitance.

The most sensitive detector-preamplifier operation results when the noise is completely dominated by the shot noise from the photodiode. This condition can only be met if the input capacitance and the upper frequency requirement allow use of a sufficiently large feedback resistor to produce negligible Johnson noise current. The following section will consider practical limits for input capacitance and photodiode dark leakage current to illustrate realizable values for the total noise current as a function of upper frequency requirement.

## EXPERIMENTAL EVALUATION

### Circuit Configuration

In order to determine the practical performance limitations of the DC mode of operation, a photodiode-preamplifier circuit was constructed, and measurements were made to evaluate photodiode responsivity, frequency response, and noise sources. Discrete components were used for the construction of the preamplifier shown in figure 5. A diffused-channel field-effect transistor (FET), which has low gate leakage current and

thus minimal shot noise current, was selected. A typical feedback resistance of  $100\text{ M}\Omega$  is shown in the circuit diagram. For any particular case, however, this value must be maximized to reduce the contribution of Johnson noise current while providing the desired frequency response. The FET is operated as a source follower to avoid multiplication of the gate-to-drain capacitance. The succeeding transistor stages keep the load impedance high on the source terminal of the FET, produce the phase reversal for negative feedback, and keep the output impedance low.

### Responsivity

A Hewlett-Packard model 5082-4205 photodiode (referred to as HP 4205) was selected since it is a small-area, low-noise device. The responsivity of the photodiode, specified in amperes per watt, was measured with a calibrated standard of irradiance, interference filters, and a pinhole aperture mounted over the photodiode, thereby providing a known incident radiant power to the photodiode. The current-to-voltage conversion of the preamplifier was specified by measuring the feedback resistance and the voltage gain. Results of the responsivity measurement are shown in figure 6 and agree with the manufacturer's data (ref. 13).

### Noise Spectrum

In order to evaluate the performance of the preamplifier under different bandwidth requirements, the noise spectrum was measured for three different values of feedback resistance. Measured noise voltages were referred back to the input in terms of noise current per root hertz for more direct comparison with the signal current. Results of the noise-current measurements are shown in figure 7 along with the theoretical Johnson noise currents for the feedback resistors used.

Measurement of the noise current at low frequencies indicates only a slight appearance of  $1/f$  noise; consequently,  $1/f$  noise does not contribute significantly to the total noise current. At higher frequencies the noise currents agree closely with the calculated Johnson noise currents, indicating that the shot noise current is not significant and therefore the photodiode leakage current is small. From figure 7 it appears that shot-noise-limited operation cannot be achieved for an upper frequency limit above a few hundred hertz because of the input capacitance and Johnson noise from the feedback resistor.

Frequency-response measurements for the three feedback resistors are listed in table I along with the calculated effective input capacitance. The  $10\text{-M}\Omega$  resistor was physically larger than the  $150\text{-M}\Omega$  and  $1500\text{-M}\Omega$  resistors, and the results indicate the effect of distributive capacitance in reducing the preamplifier frequency response. More effective shielding as well as improved layout of circuit components may provide improvement in frequency response.

TABLE I.- FREQUENCY-RESPONSE MEASUREMENTS

| Feedback resistance,<br>M $\Omega$ | Frequency response<br>(3-dB cutoff),<br>kHz | Feedback capacitance,<br>pF |
|------------------------------------|---|-----------------------------|
| 10                                 | 15  | 1.1                         |
| 150                                | 4   | .13                         |
| 1500                               | .340  | .34                         |

### PERFORMANCE EVALUATION

The performance of the circuit configuration presented here can best be evaluated by applying the experimental results to the analytical description of system sensitivity. This approach was utilized to describe the performance of the DC mode of operation in terms of detectable incident power as a function of bandwidth requirement.

For the purpose of presenting system performance, the signal current is determined by using 0.8- $\mu$ m radiation incident on the photodiode and a responsivity value of 0.37 A/W. The noise current is determined by integrating the noise spectra shown in figure 7 from a lower limit determined by operation of the drift-control circuit to an upper limit set by the 3-dB frequency. Operation of the drift-control circuit was specified under camera operating conditions of a 100<sup>o</sup> vertical field of view; a 0.1<sup>o</sup> instantaneous field of view, or angular resolution; and a Nyquist sampling rate.

Results of the calculations of signal and noise currents are illustrated in figure 8, which shows the noise-equivalent radiant power as a function of the upper frequency limit. The value shown for a frequency of 15 kHz should be improved upon by reduction of stray capacitance, as previously mentioned. The curve shown should have a slope of 1 in the region dominated by Johnson noise (300 Hz to 15 kHz), as indicated by the data points. As the bandwidth requirement is further reduced, the total noise current becomes dominated by shot noise from the photodiode and the slope approaches 1/2. The dashed portion of the curve indicates the region dominated by shot noise and was determined analytically from the manufacturer's measurements of photodiode leakage currents. The slope of the sensitivity curve must then approach zero as 1/f noise dominates; however, the dependence upon 1/f noise cannot accurately be specified because of the variation from one device to another and the low-frequency measurement capability necessary for experimental verification. Noise-spectra measurements shown in figure 7 indicate that 1/f noise does not dominate until very low frequencies are reached, which would be encountered only with very long frame times.



On the basis of the measurements of photodiode-preamplifier noise, it appears that the DC mode of operation offers excellent sensitivity for use with the facsimile camera. The more common technique of chopping the incident radiation and ac amplifying the video signal offers several disadvantages: (a) the mechanical complexity associated with chopping the radiation, (b) the loss of approximately 50 percent of the total energy incident on the photodiode, and (c) the increase by a factor of at least 3 in the necessary frequency response of the preamplifier, which introduces additional Johnson noise and decreases sensitivity. Generally, the decision to chop the radiation results when the system performance is degraded by  $1/f$  noise and drift. In the case of the facsimile camera, however, the unique scanning operation allows implementation of the DC mode of operation by sampling the  $1/f$  noise and drift and effectively reducing them from the video signal. In addition, for operation under practical bandwidth requirements, the contribution from  $1/f$  noise appears to be small, as evidenced by the experimental data presented herein. This fact further reduces the necessity for chopping in the facsimile camera and illustrates the advantage offered by the DC mode of operation.

#### CONCLUDING REMARKS

An analysis and evaluation was presented of the direct-coupled (DC) mode of silicon photodetector and preamplifier operation for generation of video data from facsimile cameras. The analysis defined system signal-to-noise ratio in terms of signal current and noise current, which is a function of required system video bandwidth. A photodiode-preamplifier configuration was presented and the noise sources were defined. Performance of the photodiode-preamplifier was experimentally evaluated, and system sensitivity was predicted for practical facsimile camera operating bandwidths.

Incorporation of a drift control technique, which samples  $1/f$  noise and drift between scan lines, allows implementation of the DC mode without serious degradation due to  $1/f$  noise and drift. The DC mode of operation utilizes all available radiant energy and offers a reduced preamplifier frequency-response requirement and a greater mechanical simplicity when compared with the more common technique of ac chopping the radiation. On the basis of these considerations, the DC mode of detector operation provides the most sensitive reliable photon detection technique for facsimile cameras.

Langley Research Center,  
National Aeronautics and Space Administration,  
Hampton, Va., July 23, 1973.

## REFERENCES

1. Huck, Friedrich O.; and Lambiotte, Jules J., Jr.: "A Performance Analysis of the Optical-Mechanical Scanner as an Imaging System for Planetary Landers. NASA TN D-5552, 1969.
2. Dostal, Frank: Light Light Choppers. *Opt. Spectra*, vol. 2, issue 2, Mar.-Apr. 1968, pp. 29-32.
3. Jamieson, John A.; McFee, Raymond H.; Plass, Gilbert N.; Grube, Robert H.; and Richards, Robert G.: *Infrared Physics and Engineering*. McGraw-Hill Book Co., Inc., c.1963.
4. Sawyer, D. E.; and Rediker, R. H.: Narrow Base Germanium Photodiodes. *Proc. IRE*, vol. 46, no. 6, June 1958, pp. 1122-1130.
5. Philipp, H. R.; and Taft, E. A.: Optical Constants of Silicon in the Region 1 to 10 eV. *Phys. Rev.*, second ser., vol. 120, no. 1, Oct. 1, 1960, pp. 37-38.
6. Eng. Staff of Philbrick/Nexus Res.: *Applications Manual for Operational Amplifiers*. Teledyne Co., Aug. 1969.
7. Kruse, Paul W.; McGlauchlin, Laurence D.; and McQuistan, Richmond B.: *Elements of Infrared Technology*. John Wiley & Sons, Inc., 1963.
8. Gray, Paul E.; DeWitt, David; Boothroyd, A. R.; and Gibbons, James F.: *SEEC Notes 2 - PEM: Physical Electronics and Circuit Models of Transistors*. John Wiley & Sons, Inc., c.1963.
9. Bennett, William R.: *Electrical Noise*. McGraw-Hill Book Co., Inc., 1960.
10. Sevin, Leonce J., Jr.: *Field-Effect Transistors*. McGraw-Hill Book Co., Inc., c.1965.
11. Smith, Lewis; and Sheingold, D. H.: *Noise and Operational Amplifier Circuits*. *Analog. Dialogue*, vol. 3, no. 1, Mar. 1969.
12. Katzberg, Stephen J.; Kelly, W. Lane, IV; Rowland, Carroll W.; and Burcher, Ernest E.: *Design and Evaluation of Controls for Drift, Video Gain, and Color Balance in Spaceborne Facsimile Cameras*. NASA TN D-7333, 1973.
13. Anon.: PIN Photodiode. HP 5082-4200 Series, Hewlett Packard, Oct. 1, 1968.

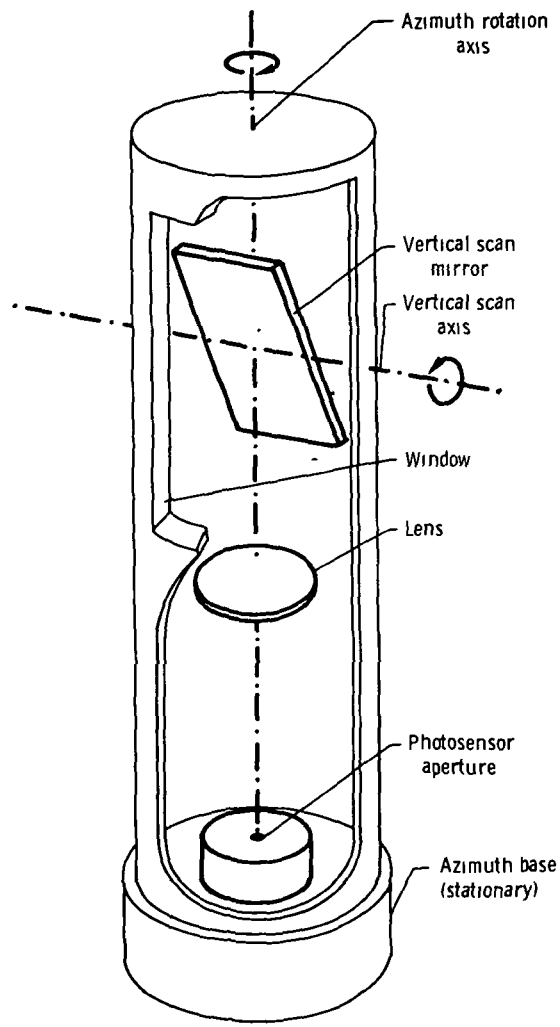


Figure 1. - Basic facsimile camera configuration.

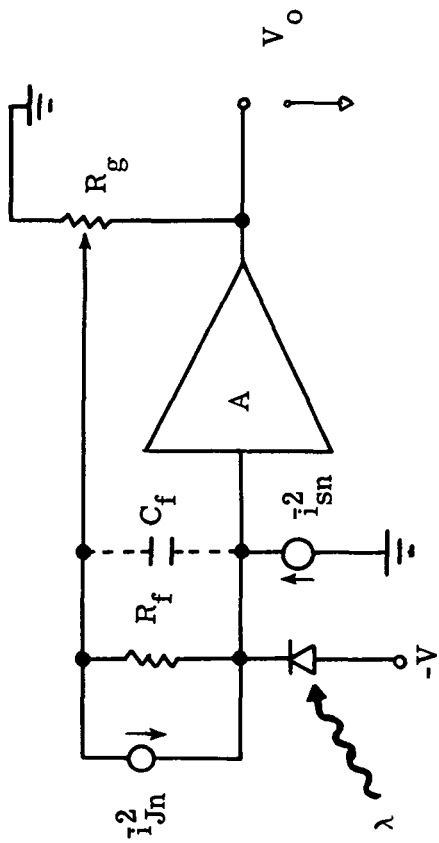


Figure 2.- Model of preamplifier circuit.

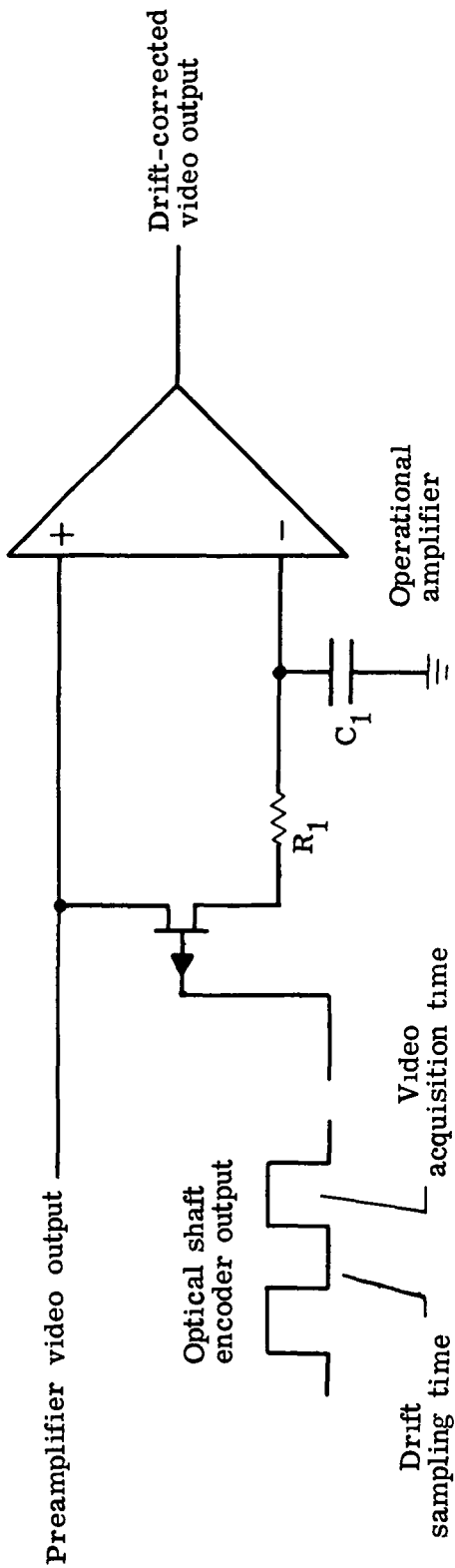


Figure 3.- Drift-control circuitry.

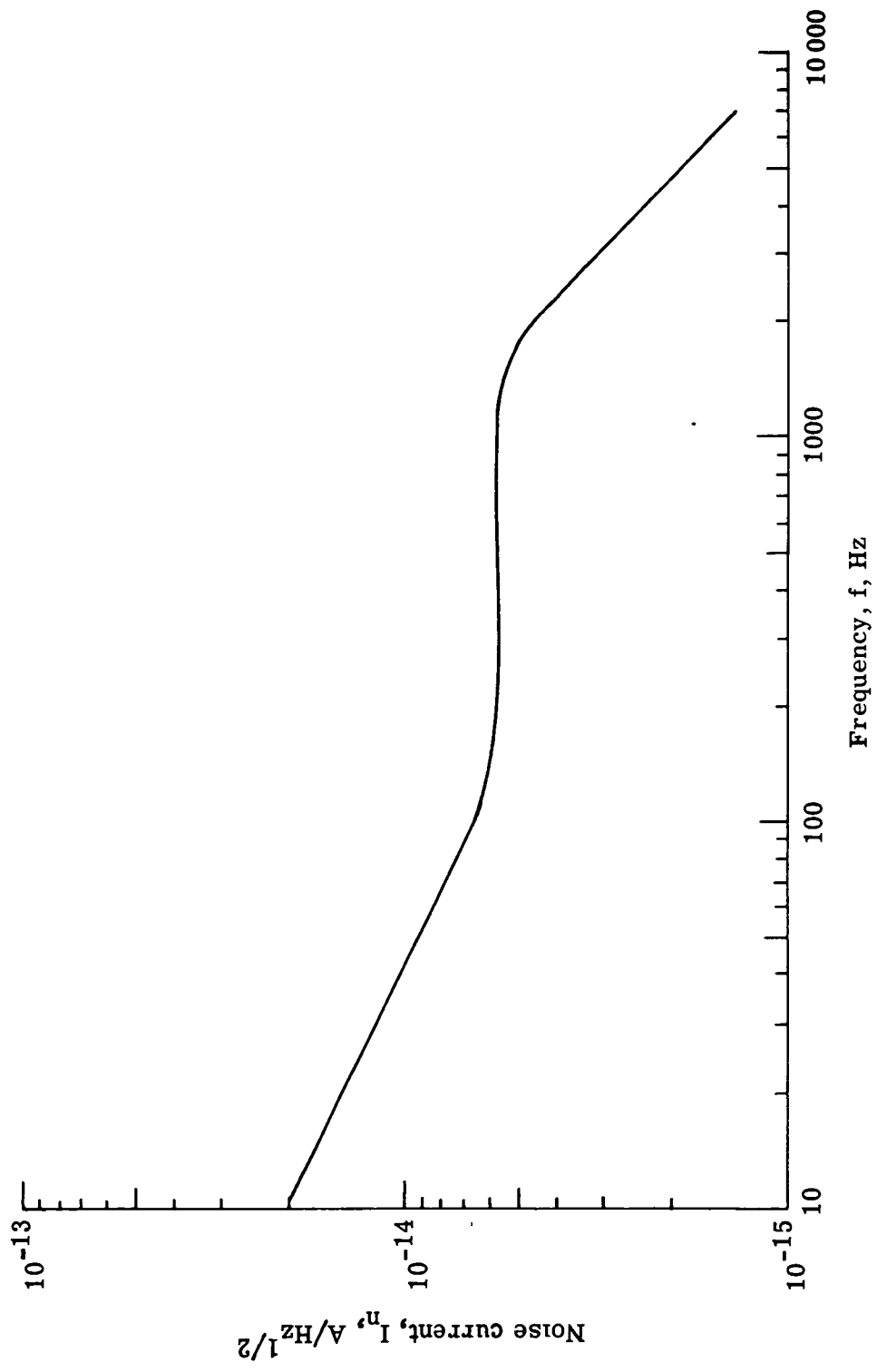


Figure 4.- Typical noise-density spectrum of photodiode-preamplifier.

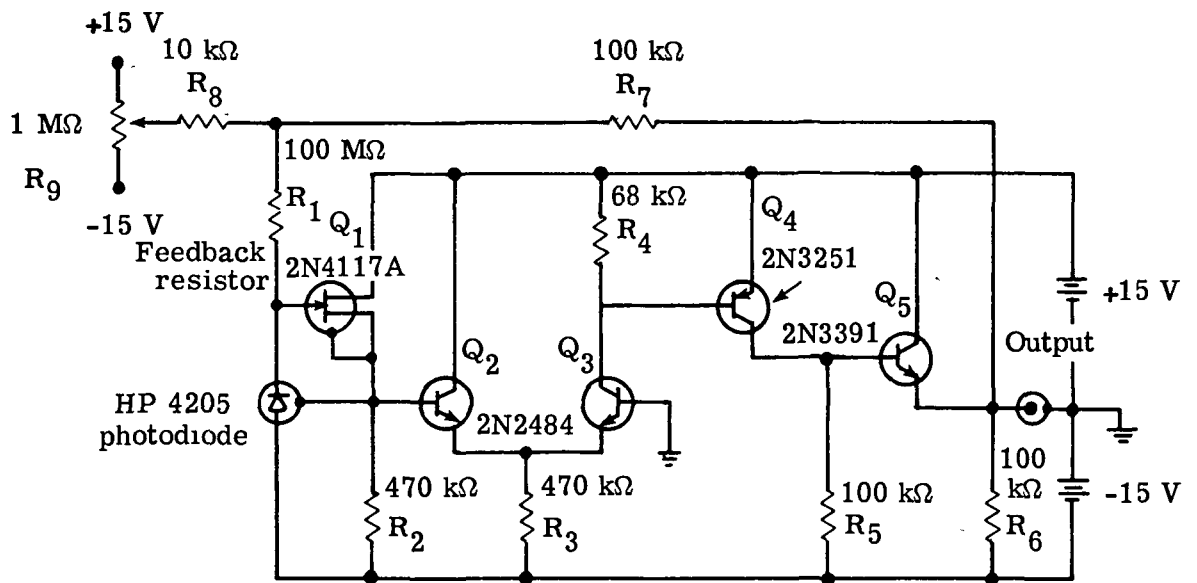


Figure 5.- Schematic of detector-preamplifier.

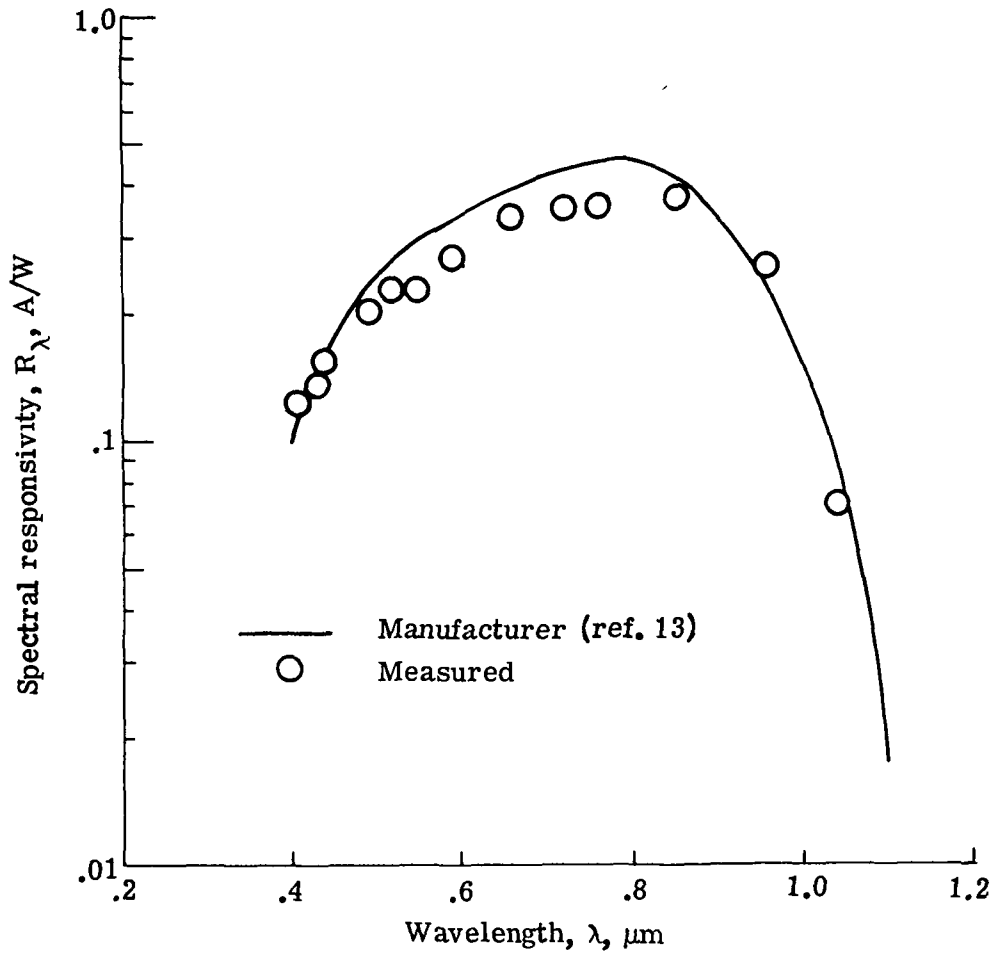


Figure 6.- Spectral responsivity of silicon PIN HP 4205 photodiode.

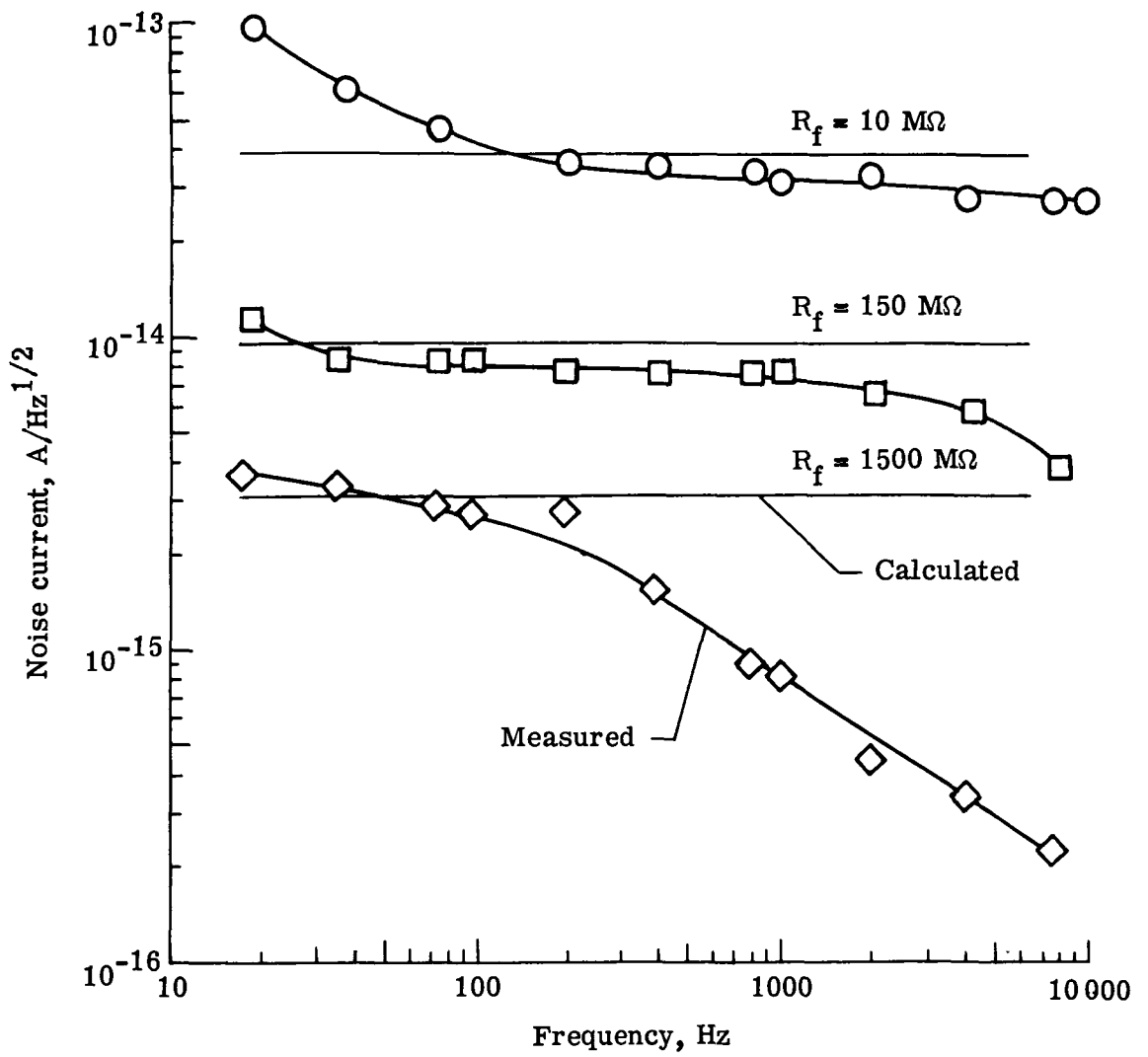


Figure 7.- Measured noise spectra for three feedback resistances.



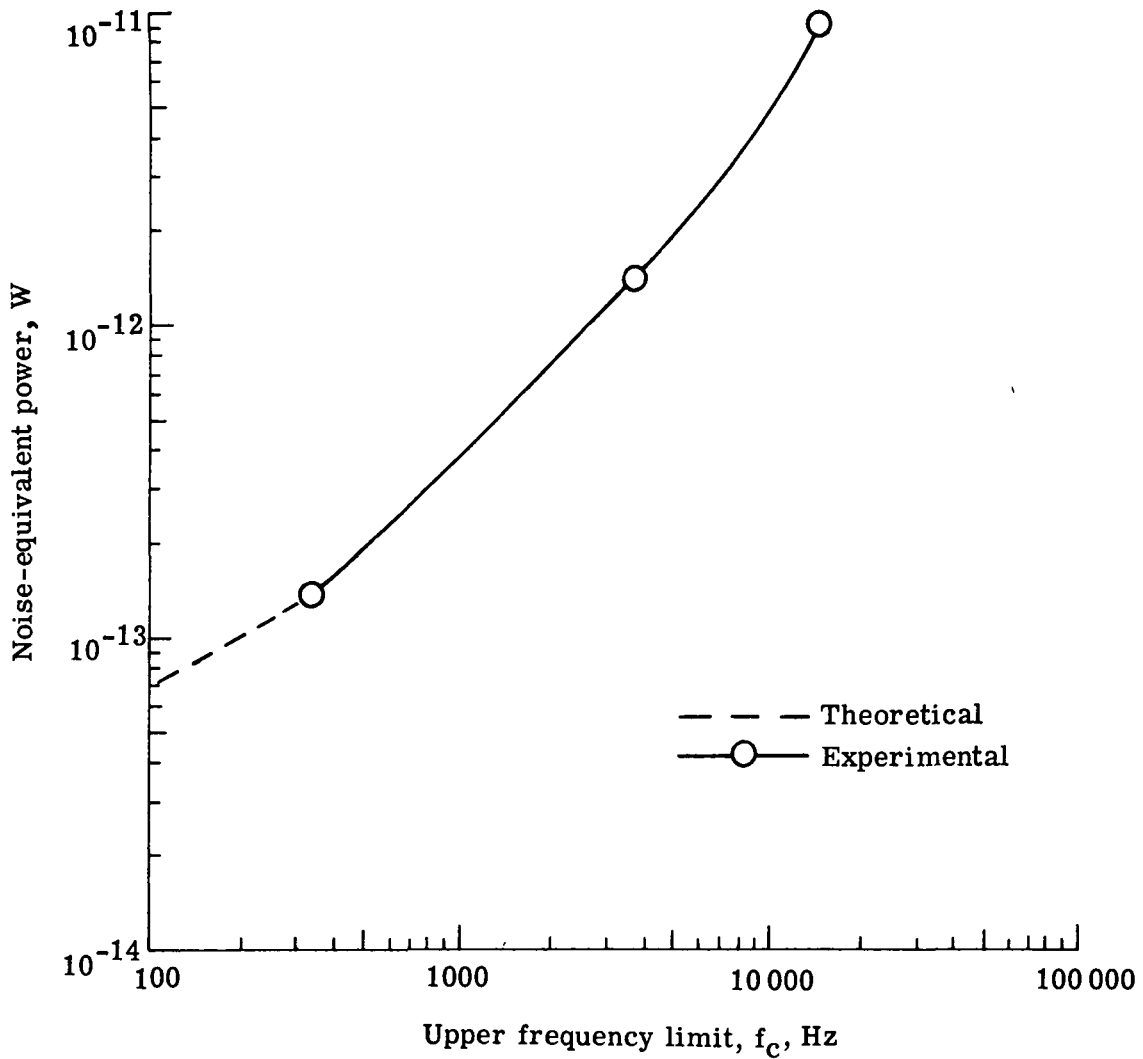


Figure 8.- Noise-equivalent power at  $\lambda = 0.8 \mu\text{m}$  as a function of upper frequency limit.



POSTMASTER

If Undeliverable (Section 158  
Postal Manual) Do Not Return

*"The aeronautical and space activities of the United States shall be conducted so as to contribute . . . to the expansion of human knowledge of phenomena in the atmosphere and space. The Administration shall provide for the widest practicable and appropriate dissemination of information concerning its activities and the results thereof."*

—NATIONAL AERONAUTICS AND SPACE ACT OF 1958

## NASA SCIENTIFIC AND TECHNICAL PUBLICATIONS

**TECHNICAL REPORTS** Scientific and technical information considered important, complete, and a lasting contribution to existing knowledge

**TECHNICAL NOTES** Information less broad in scope but nevertheless of importance as a contribution to existing knowledge

**TECHNICAL MEMORANDUMS** Information receiving limited distribution because of preliminary data, security classification, or other reasons. Also includes conference proceedings with either limited or unlimited distribution.

**CONTRACTOR REPORTS** Scientific and technical information generated under a NASA contract or grant and considered an important contribution to existing knowledge

**TECHNICAL TRANSLATIONS** Information published in a foreign language considered to merit NASA distribution in English

**SPECIAL PUBLICATIONS** Information derived from or of value to NASA activities. Publications include final reports of major projects, monographs, data compilations, handbooks, sourcebooks, and special bibliographies

**TECHNOLOGY UTILIZATION PUBLICATIONS** Information on technology used by NASA that may be of particular interest in commercial and other non-aerospace applications. Publications include Tech Briefs, Technology Utilization Reports and Technology Surveys

**Details on the availability of these publications may be obtained from:**

**SCIENTIFIC AND TECHNICAL INFORMATION OFFICE**

**NATIONAL AERONAUTICS AND SPACE ADMINISTRATION**

**Washington, D.C. 20546**